Oil & Natural Gas Technology

DOE Award No.: DE-FE0010496

Quarterly Research Performance Progress Report

(Period ending 01/31/14)

Application of Crunch-Flow Routines to Constrain Present and Past Carbon Fluxes at Gas-Hydrate Bearing Sites

Project Period: October 1, 2012 – January 31, 2014

Submitted by:
Marta Torres
Professor of Oceanography
Oregon State University
DUNS #: 053599908
104 COAS Admin. Bldg.
Corvallis, OR 97331-5503
e-mail: mtorres@coas.oregonstate.edu
Phone number: (541) 737-2902

Prepared for:
United States Department of Energy
National Energy Technology Laboratory

11 February 2014

Office of Fossil Energy

EXECUTIVE SUMMARY

In November 2012, Oregon State University initiated the project entitled: **Application of Crunch-Flow routines to constrain present and past carbon fluxes at gas-hydrate bearing sites.** This project aims to develop a modeling module that will include all important biogeochemical processes that need to be considered in a cold seep environment. This module will be applied on several DOE-supported drilling expeditions (e.g., Cascadia margin in US, Ulleung Basin in South Korea, and K-G basin in India) to quantify the dynamics of methane at present day and in the past.

We have completed a model that provides quantitative estimates of the thickness of individual mass transport deposits (MTDs), time elapsed after the MTD event, rate of sulfate reduction in the MTD, and time required to reach a new steady state at several sites drilled in the Krishna-Godavari (K-G) Basin off India. In addition we developed a hybrid model scheme by coupling a home-made MATLAB code with CrunchFlow to address the methane transport and chloride enrichment at the Ulleung Basins chimney sites, and contributed the modeling component to a study focusing on pore-scale controls on gas hydrate distribution in sediments from the Andaman Sea. These efforts resulted in one manuscripts currently under review, and contributed the modeling component of another pare, also under review. Lessons learned from these efforts are the basis of a mini-workshop to be held at Oregon State University (Feb 2014) to instruct graduate students (OSU and UW) as well as DOE staff from the NETL lab in Albany on the use of Crunch Flow for geochemical applications.

PROGRESS, RESULTS, AND DISCUSSION

1. Gas hydrate and methane transport in Ulleung Basin.

The primary goal of this project is to develop a model scheme that can simulate gas hydrate dissociation, dissolution, and formation in the shallow sediments of Ulleung Basin. This model can be constrained by pore water Cl profiles from this basin, where positive anomalies of Cl (up to 1400 mM) was observed from the depth as shallow as 25 mbsf. Cl is considered as an inert tracer since it is free from most of the biogeochemical reactions and reflects only transport processes and the amount of water in the sediments. We intended to develop the model scheme by using CrunchFlow, which was used throughout this project to simulate various biogeochemical reactions in the sediments. However we discovered that CrunchFlow alone is not capable of dealing with this topic as some of the important properties (e.g., temperature, permeability, porosity, and Darcy velocity) are not time-dependent. CruchFlow is still attractive to attain our project goal because of its full capability in dealing with biogeochemical reactions and its very efficient built-in mathematical engine to solve the partial differential equations. We therefore developed a hybrid model scheme by coupling a home-made MATLAB code with CrunchFlow. The MATLAB code is used to calculate all reactions and the corresponding changes in sediment and fluid properties, whereas CrunchFlow will be used to redistribute chemical species based on their transport behaviors. Such scheme will provide us the flexibility we need for our task while we can still take advantage of the computational capability and geochemistry database in CrunchFlow. Description of the model architecture and results is given in Appendix 1.

2. **Effect of mass transport deposits on pore water profiles in the Krishna-Godavari Basin, India**. Mass transfer deposits (MTDs) in the Krishna-Godavari Basin on the eastern Indian margin are common sedimentary features over the modern continental slope. Quantitative understanding of the scale and age of these MTDs is especially important when studying their trigger-

ing mechanisms and environmental feedbacks, and is also important for interpreting pore fluid chemical profiles. Pore water profiles in sediments recovered during the 2006 Indian National Gas Hydrate Project (NGHP-01) expedition suggest that MTDs are present at seven of the sites cored in the Krishna-Godavari Basin. Kinetic modeling of the S-shaped pore water sulfate profiles as well as the pore water ammonium profiles from these sites provides quantitative estimates of the thickness of individual MTDs, time elapsed after the MTD event, rate of sulfate reduction in the MTD, and time required to reach a new steady state. The model results suggest that the MTDs at the seven study sites are 8 to 25 meters thick and 300 to 1600 years old. Within the MTD sections, sulfate reduction rates are 126 to 1215 mmol/m^{2}yr. In comparison to depth-integrated sulfate reduction rates estimated in other regions, our estimates are relatively high reflecting a much thicker sulfate reduction zone as a result of the MTDs. A positive correlation is observed between water depth and the sedimentation rate in the MTD sections (i.e., thickness of MTD divided by its age), which agrees with previous studies of MTDs in this region. We caution against using the pore water profiles of sites experiencing significant MTDs to infer metabolic processes and to quantify steady-state reaction rates as our model results confirm the remarkable influence of transient MTDs on pore water profiles. Results of this effort are given on a manuscript that will be submitted for publication as part of the JPMG special issue on gas hydrates results from the NGHP-01 drilling project offshore India, and is given in Appendix 2.

CONCLUSION

We have applied the kinetic models developed previously in the context of this work to quantify the role of sediment mass transport in the carbon cycle at gas hydrate bearing sites is the quantification of mass transport events in sediments from the Krishna-Godavari basin. We also developed a hybrid model that that couples a MATLAB code with CrunchFlow. The MATLAB code is used to calculate all reactions and the corresponding changes in sediment and fluid properties, whereas CrunchFlow will be used to redistribute chemical species based on their transport behaviors. With such a scheme we are able to simulate the Cl anomalies in the Ulleung basin, and provide constraints as to the timing of the methane fluxes.

MILESTONE STATUS

All Milestones are completed

PRODUCTS

→ This l report

→ Submitted a manuscript entitled “A kinetic-model approach to quantify the effect of mass transport deposits on pore water profiles in the Krishna-Godavari Basin, Bay of Bengal” byWei-Li Hong, Evan Solomon, and Marta Torres for publication in the JMPG Special Results volume focusing on NGHP-01 results

→ A mini-workshop to be held at OSU, with the purpose of training graduate students and researchers from NETL in the use of Crunch Flow to model geochemical processes.

PROBLEMS OR DELAYS

None

Appendix 1

Dynamic of gas hydrate and transport of methane gas in Ulleung Basin

Dynamic of gas hydrate and transport of methane gas in Ulleung Basin

Abstract

The primary goal of this project is to develop a model scheme that can simulate gas hydrate dissociation, dissolution, and formation in the shallow sediments of Ulleung Basin. This model can be constrained by pore water Cl profiles from this basin, where positive anomalies of Cl (up to 1400 mM) was observed from the depth as shallow as 25 mbsf. Cl is considered as an inert tracer since it is free from most of the biogeochemical reactions and reflects only transport processes and the amount of water in the sediments. We intended to develop the model scheme by using CrunchFlow, which was used throughout this project to simulate various biogeochemical reactions in the sediments. However we discovered that CrunchFlow alone is not capable of dealing with this topic as some of the important properties (e.g., temperature, permeability, porosity, and Darcy velocity) are not time-dependent. CruchFlow is still attractive to attain our project goal because of its full capability in dealing with biogeochemical reactions and its very efficient built-in mathematical engine to solve the partial differential equations. We therefore developed a hybrid model scheme by coupling a home-made MATLAB code with CrunchFlow. The MATLAB code is used to calculate all reactions and the corresponding changes in sediment and fluid properties, whereas CrunchFlow will be used to redistribute chemical species based on their transport behaviors. Such scheme will provide us the flexibility we need for our task while we can still take advantage of the computational capability and geochemistry database in CrunchFlow. A preliminary version of this model has been built to simulate the chloride profile at UBGH2-3. To fit the profile, transport of free gas methane is essential which agrees with previous observations.

Project goal overview

The primary goal of this project is to develop a model scheme that can simulate gas hydrate dissociation, dissolution, and formation in the shallow sediments of Ulleung Basin. This model will be constrained by pore water Cl profiles from this basin, where positive anomalies of Cl (up to 1400 mM) was observed from the depth as shallow as 25 mbsf. Cl is considered as an inert tracer since it is free from most of the biogeochemical reactions and reflects only transport processes and the amount of water in the sediments. We intent to develop the model scheme by using CrunchFlow, which was used throughout this project to simulate various biogeochemical reactions in the sediments. We however discovered that CrunchFlow may be incapable of dealing with such topic as some of the important properties (e.g., temperature, permeability, porosity, and Darcy velocity) are not time-dependent. CruchFlow is still attractive to our project goal due to its full capability in dealing with biogeochemical reactions and very efficient built-in mathematical engine to solve the partial differential equations. We therefore developed a hybrid model scheme by coupling a home-made MATLAB code with CrunchFlow. The MATLAB code will be used to calculate all reactions and the corresponding changes in sediment and fluid properties whereas CrunchFlow will be used to redistribute chemical species based on their transport behaviors. Such scheme will provide us the flexibility we need for our task while we can still take advantage of the computational capability and geochemistry database in CrunchFlow.

The hybrid model scheme

The entire model scheme consists of two parts: the set-up for initial environment and the looping between MATLAB and CrunchFlow. The sequence of this hybrid model scheme is illustrated in Figure 1 and detailed in the following paragraphs.

Initial setup of the sediment and fluid properties (Figure 1a)

The MATLAB code reads the initial condition assigned to CrunchFlow and uses it to calculate the initial value for the properties such as liquid saturation, porosity, formation temperature, Darcy velocities for fluid and gas, and permeability. As CurnchFlow calculates only the partial pressure of gases, we need to assume an initial volume of gas (10^{-5} m3/m3). The volume of gas, together with the porosity, is used to calculate the fraction of each phase (water, gas, hydrate, and sediments). The liquid saturation can then be calculated from the fraction of gas and water. Permeability is calculated based on liquid saturation and the fractions of sediment grain and hydrate. Pressure of water phase, which is needed to calculate the density of gas, can be derived from the ambient pressure (hydrostatic pressure), liquid saturation, and density of pore water (assumed to be seawater initially). The Darcy velocities for water and gas can be computed from many of the aforementioned information. Liquid saturation, porosity, formation temperature, Darcy velocities for fluid and gas, and permeability are then feed to CrunchFlow for next step.

Setup of the CrunchFlow environment (Figure 1b)

With the information calculated from the previous step, a CrunchFlow simulation is initiated by considering dissolved chloride, sodium, and methane in the pore water as well as gaseous methane and gas hydrate. The CrunchFlow code reads in information of sedimentation rate, liquid saturation, porosity, formation temperature, Darcy velocities for fluid and gas, and permeability and redistribute chemical species based on laws of diffusion and advection of fluid and gas. We now assumed constant formation factor, but this could potentially be time-dependent if a proper link with the abundance of hydrate is mathematically described. CrunchFlow then outputs the resulting concentration profiles of all species from different phases (i.e., water, gas, and solid).

Reassessment of the sediment and fluid properties (Figure 1c)

The new distribution of chemical species among different phases is used by the MATLAB code to update the fraction of the four phases. Reaction rates of hydrate formation, hydrate dissociation, hydrate dissolution, and gas dissolution are calculated based on the updated phase fractions. As hydrate and methane gas appear (or disappear), the densities, pressures, and the Darcy velocities of gas and water will change accordingly, as well as the formation temperature. Many of these properties are mutually dependent. For example, pressure of water is a function of water density, chloride content, and formation temperature. The density of water depends on the density of gas which is a function of water pressure. To solve these mutually depended parameters, a Newton-Raphson iterative scheme is implemented.

Preliminary model results

A preliminary version of the model has been built which allows reactions and transport can be calculated separately. This version, however, the update of sediment and fluid properties (e.g., Darcy flow, permeability, temperature, density) in the modeling loop has not yet been included due to some numerical issues. We simulated the pore water chloride profile at site UBGH2-3 with this preliminary model (Figure 2). In order to fit the chloride profile, transport of gas form of methane is essential. This conclusion agrees with the conclusion by Torres et al. (2004) in Hydrate Ridge.

Figure 1: The hybrid model scheme

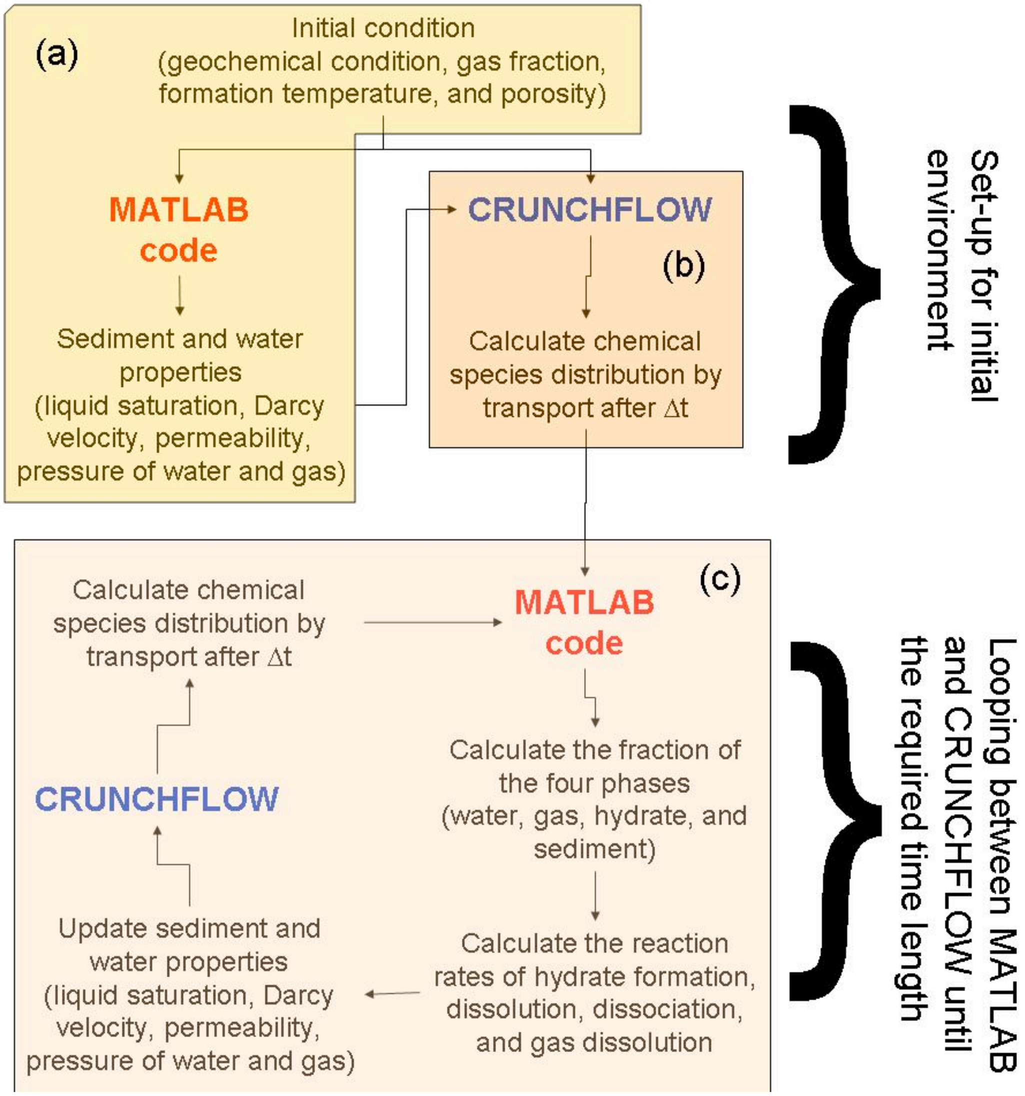

Figure 2: Model fitting with chloride data from UBGH2-3

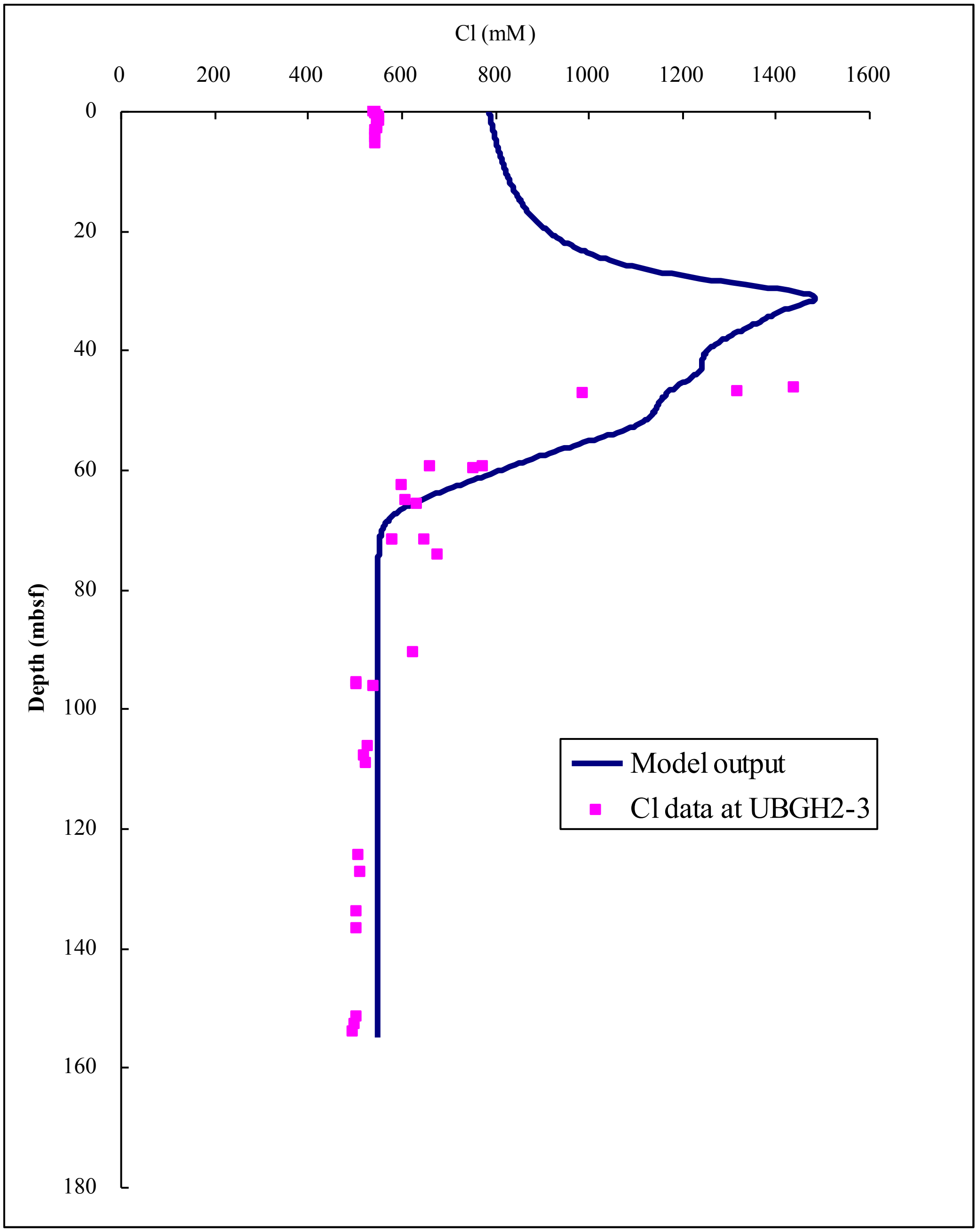

Appendix 2

A kinetic-model approach to quantify the effect of mass transport deposits on pore water profiles in the Krishna-Godavari Basin, Bay of Bengal

A kinetic-model approach to quantify the effect of mass transport deposits on pore water profiles in the Krishna-Godavari Basin, Bay of Bengal

Wei-Li Hong[1], Evan Solomon[2], Marta Torres[1]

[1] College of Earth, Ocean, and Atmospheric Sciences, Oregon State University, 104 CEOAS administration bldg, Corvallis, OR 97331, USA.

[2] School of Oceanography, University of Washington, Seattle, WA 98195

Abstract

Mass transfer deposits (MTDs) in the Krishna-Godavari Basin on the eastern Indian margin are common sedimentary features over the modern continental slope. Quantitative understanding of the scale and age of these MTDs is especially relevant to understanding their triggering mechanisms and environmental feedbacks, as well as for interpreting pore water chemical profiles. Pore water profiles in sediments recovered during the 2006 Indian National Gas Hydrate Project (NGHP-01) expedition suggest that MTDs are present at seven of the sites cored in the Krishna-Godavari Basin. Kinetic modeling of the S-shaped pore water sulfate and ammonium profiles from these sites provides quantitative estimates of the thickness of individual MTDs, time elapsed after the MTD event, rate of organic matter-fueled sulfate reduction in the MTD, and time required to reach a new steady state. The model results suggest that the MTDs at the seven study sites are 8 to 25 meters thick and are 300 to 1600 years old. Within the MTD sections, the organic matter-fueled sulfate reduction rates are 126 to 1215 mmol/m^2/yr and the time needed to reach a new steady state ranges from 2000 to 3800 years. In comparison to depth-integrated sulfate reduction rates estimated in other regions, our estimates are relatively high reflecting a much thicker sulfate reduction zone that results from the MTDs. A positive correlation is observed between water depth and the sedimentation rate in the MTD sections (i.e., thickness of MTD divided by its age), which agrees with previous studies of MTDs in this region. We caution against using the pore water data from sites experiencing significant MTDs to infer metabolic processes and to quantify steady-state reaction rates as our model results confirm the remarkable influence of transient MTDs on pore water profiles.

Introduction

The Krishna-Godavari (K-G) Basin on the eastern Indian margin is characterized by extensive mass-transport deposits (MTDs) formed by sliding/slumping of river-delivered sediments (Forsberg et al., 2007; Ramana et al., 2009: Shanmugam et al., 2009; Ramprasad et al., 2011). MTDs in the K-G Basin may be related to variations in regional climate and changes in sediment discharge from the Krishna and Godavari rivers (Forsberg et al., 2007; Ramana et al., 2009; Ramprasad et al., 2011). However, the regional variability, magnitude, and age of the individual events are poorly constrained. Furthermore, sediments deposited by these abrupt events likely alter the pore water geochemical records in the shallow sediments, and hinder development of quantitative models for early diagenetic processes in this margin.

Pore water composition is very sensitive to localized and recent slumping events, as previously shown by Hensen et al. (2003) and Holsein and Wirtz (2010). The pore water profiles sampled during the recent Indian National Gas Hydrate Project (NGHP-01) expedition (Figure 1) provide a unique opportunity to quantify the timing and magnitude of these deposits. In this study, we apply a transport-reaction model to pore water data from seven sites drilled in the K-G basin (Table 1) to quantify the thickness of the deposits and the time elapsed after each event. This information is potentially important for future studies focusing on the control and/or feedback mechanisms of these episodic sediment transport events. Our work also highlights the importance of these events on the shape of pore water solute profiles and on their interpretation.

Study region

The modern K-G Basin in the eastern passive margin basin of India receives large sediment inputs from the Krishna and Godavari Rivers. The delta fronts exhibit MDTs, scars and irregular topography over the modern upper continental slope formed by sliding/slumping (Forsberg et al., 2007; Ramana et al., 2009; Ramprasad et al., 2011). Sediments transported through large canyons also contribute to the total sediment accumulations (Kotha, 2002; Bastia, 2004; Murthy, 1999). Recent seismic and bathymetric surveys in this area imaged widespread MTDs (Solheim et al., 2007; Forsberg et al., 2007; Shanmugam et al., 2009; Ramprasad et al., 2011), and were used to guide drilling during the NGHP-01 expedition in 2006.

Sediment thickness in the K-G basin varies from 3 to 5 km and may exceed 8 km in the offshore region (Prabhakar and Zutshi, 1993). Drilling during NGHP-01 sampled the upper 200-300 meters at 15 sites, aimed at characterizing the gas hydrate potential of this region (Figure 1). Here we focus only on the first 40-60 meters of the sediment column (Table 2), in an effort to unravel the relative magnitude and frequency of slumping events, as their effect on pore water profiles impact ongoing efforts to quantify organic carbon cycling and methane dynamics in this passive margin (Solomon et al., this issue). The sediments studied all correspond to the same Quaternary lithostratigraphic unit primarily composed of clay with variable amounts of carbonates (4-60%), and trace amounts of quartz, feldspar, mica, and iron sulfide (Collett et al., 2008). Frequent silt/sand beds are observed at each site (Collett et al., 2008). The distribution of authigenic carbonate is not necessarily correlated with the current sulfate-methane-transition-zone (SMTZ), defined by the pore water sulfate and methane profiles, suggesting migration of the SMTZ in the past (Collett et al., 2008) or simply burial of authigenic carbonates produced at the SMTZ through time, perhaps punctuated by sediment slumping.

Effect of MTDs on the pore water data

Shipboard pore water analyses, including sulfate concentration, were reported in Collett et al. (2008). Shorebased pore water ammonium analyses were reported in Solomon et al. (this issue). Pore water profiles in seven of the 15 sites drilled in the K-G Basin suggest a non-steady-state condition (Figure 2). The concentration of all pore water species, especially sulfate, at these seven sites changes rapidly in a relatively short depth interval, indicating the importance of non-diffusional processes. A rapid drop in sulfate content and the concordant increases of both ammonium and dissolved inorganic carbon (DIC) concentrations at the first ~5 meters in the sediments (Collett et al., 2008; Solomon et al., this issue) are indicative of sulfate consumption due to organic matter degradation (abbreviated as POCSR, particulate organic carbon sulfate reduction, hereafter). As no methane present in this interval, POCSR should be the only reaction consuming sulfate. Between 15 to 25 meters below seafloor (mbsf), sulfate content remains constant until it is again consumed by methane through anaerobic oxidation of methane (AOM) and POCSR at greater depths (Figure 2). We hypothesize that these sulfate profiles reflect recent mass transfer events at each site, and that the slumping is too recent for diffusion to smooth the dissolved sulfate distribution between the two sulfate reduction zones.

Before slumping, sulfate supplied by diffusion from overlying seawater is consumed by both POCSR and AOM, which forms a distinct SMTZ (Figure 2A). In environments devoid of slumping these processes act together to generate a smooth decrease in dissolved sulfate with depth (e.g., Claypool and Kaplan, 1974; Froelich et al., 1979; Borowski et al., 1999; Hong et al., 2013; Figure 2A). If then a layer of sediment with fresh labile organic matter is rapidly deposited by a MTD (Figure 2B), the SMTZ is buried deeper while the reactive organic matter in the newly deposited sediments also consumes sulfate, leading to the shallow-most drop in sulfate content and effectively separating both sulfate consuming processes (Figure 2C). This produces the S-shaped profiles observed and clearly indicates that the system is out of steady state. Eventually, the persistent bottom methane supply will move the SMTZ upward until a new steady state is reached (Figure 2D). We use a kinetic modeling approach to explore the conditions leading to the S-shape of sulfate profiles from these seven sites to unravel the effects of MTDs on pore water geochemistry.

Model architecture

Reaction formulation

In these simulations we use the FORTRAN routine CrunchFlow, as described in Steefel (2009). Hong et al. (2013; 2014) has listed the various reactions involved around the SMTZ, among which we focus only on POCSR and AOM. Above SMTZ, where there is no methane present, POCSR is responsible for all of the sulfate consumption; AOM becomes more significant closer to the SMTZ. These two reactions can be summarized as:

$$(CH_2O)(NH_3)_{\frac{x}{106}}(H3PO4)_{\frac{1}{106}} + 0.5SO_4^{-2} + (0.01886 - \frac{x}{106})H^+$$

$$\rightarrow 0.5H_2S + HCO_3^- + \frac{x}{106}NH_4^+ + 0.00943HPO_4^{-2} \quad (1)$$

$$CH_4^+ + SO_4^{-2} \rightarrow HS^- + HCO_3^- + H_2O \qquad (2)$$

where x is the stoichiometry of nitrogen in the organic matter and was calculated from the C/N ratio at each site (Table 3; data from Phillips and Johnson, this volume). We aware that such calculation maybe an oversimplification, as the amount of ammonium released from organic matter degradation depends on the C/N ratio in the pool of reactive carbon instead of the bulk organic matter. However, the good agreement with the NH_4 data, as we will show later, indicates that this is still a reasonable approximation.

In order to constrain the rate of organic matter degradation in the first sulfate reduction zone (Figure 2C), we simulate pore water ammonium, which can be described as a function of both organic matter degradation and ion exchange on mineral surfaces (Von Breymann et al., 1988a, 1988b, 1990; Wallmann et al., 2006; 2008). To formulate ion exchange with CrunchFlow, we chose the *Gaines-Thomas* activity convention and specify a cation exchange capacity for the bulk sediment. Solid density is calculated based on the sum of mineral volume fractions. In the K-G Basin, ~80-90% of the sediment is composed of clay minerals (Collett et al., 2008), ~50-80% of which is smectite (Venkatarathnam and Biscaye, 1973; Pattan et al., 2008; Underwood, pers. comm.). Using a CEC for smectite of 80-150 meq/100 g of sediment (Hang and Brindley, 1970; Jaynes and Bigham, 1986), we estimated the CEC of K-G Basin sediments to range from 32 to 80 meq/100 g of sediment. The values used at each site were further constrained by data fitting using pore water measurements, and are specified for each site in Table 2.

POCSR was formulated as Monod-type reaction with one Monod term (half saturation constant of 100 μM for sulfate was adopted; Wegener and Boetius, 2009). AOM was formulated as a double-Monod-type kinetic reaction with (half-saturation constants of 500 μM were used, Wegener and Boetius, 2009). Detailed formulation for the reactions is given in Hong et al. (2014). The *Dirichlet*-type boundary conditions were used for all species, including methane. A fixed concentration of methane was assigned at the bottom of the simulation frame at each site (L in Figure 2 and Table 2). This concentration is constrained by the observed methane and sulfate profiles as this bottom supply of methane induces AOM at a rate, together with POCSR, that lead to the observed methane and sulfate profiles. It is important to notice that the observed methane concentration can only partly constrain (i.e., as minimum constraint) the model as the onboard measurements of gas concentration always suffer from gas lost when the in-situ pressure is higher than atmospheric level.

Model logistics

The sediment depth modeled (L in Figure 2) varies from site to site and was determined based on its dissolved sulfate profile (Table 2). In order to constrain the thickness of each MTD (Δx in Figure 2B) and the time elapsed since deposition (Δt_1 in Figure 2C), we evolved the model simulation in two steps. In the first step (Figure 2A), we used bottom seawater composition as the initial condition. We used a sediment deposition rate at all sites of 0.15 meter per thousand years, based on estimates listed in Collett et al., (2008) and Mazmudar et al. (2009). Giosan (pers. comm., 2009) has reported variations in sedimentation rates among the different sites ranging from 0.15 m/kyr at Site 10 to 0.85 m/kyr at Site 5. A range of sedimentation rates was therefore used to test its influence on the model results. We observed no significant effect when varying sedimentation rates from 0.15 to 0.85 m/kyr, which is not surprising since the time scale considered in this study is only on the order of several thousand years. The time length for the first step was calculated by dividing the modeled depth of each sediment column, L, by the sedimentation rate of 0.15 m/kyr. The resulting time spans (200 to 400 kyrs) are long enough for sulfate profiles to reach steady state. The assigned reactivity for organic matter and minerals (e.g., calcite and pyrite) were kept constant among all sites. We adjusted bottom methane flux to match the observed sulfate and methane gradients at the lower sections of the profiles. After this time span, when the system has reached steady state, we add an instantaneous sediment layer with a thickness denoted as Δx (Figure 2B).

The second step of model was initiated from the steady state conditions and SMTZ depths established during the first step with a new instantly deposited layer of sediments (i.e., the MTD) bearing fresh and reactive organic matter and sea water sulfate content of 28 mM (Figure 2B). From these initial conditions, we let the model evolve until it fits the observed pore water profiles. The thickness of this organic matter rich layer (Δx in Figure 2B) can be estimated by simulating the pore water sulfate profiles. The amount of time required to reach the current observed profile (Δt_1 in Figure 2C) provides an indication of the time spanned since the MTD at each site. The assigned bottom methane supply was kept constant between the two steps.

Porosity, formation factor, and formation temperature

Diffusion rates of sulfate and ammonium are the most important parameters in this model assessment. To provide a realistic estimate of the diffusion rates, the porosity, tortuosity and the in-situ temperature of sediments need to be thoroughly considered. The porosity profile at each site was obtained by fitting the observed profiles (Collett et al., 2008) with the equation for depth-dependent porosity (Boudreau, 1997):

$$\phi(z) = \phi_f + (\phi_0 - \phi_f)\exp(\gamma z) \quad (3)$$

where ϕ_f and ϕ_0 are the asymptotic porosity and porosity at the water-sediment interface, respectively. γ is an empirical constant obtained from data-fitting of the depth interval that covers the modeled depth (i.e., L in Figure 2). These parameters are reported in Table 2.

In order to account for the different diffusivities of solutes in pure fluid and porous media, a tortuosity value is required to adjust the diffusion coefficients in non-porus medium. One way to quantify the effect of tortuosity is by calculating the formation factor (FF) from resistivity log, which tracks current flow to analogue fluid transport in the porous medium. In CrunchFlow, this can be included by providing a parameter named cementation factor (*m*), which can be calculated using the FF data calculated from resistivity logs obtained from logging while drilling (LWD) and shipboard laboratory measurements with a four-pin Wenner array and a temperature probe (Collett et al., 2008). The *m* values calculated for each site through Archie's law (Steefel, 2009):

$$FF = \phi(z)^{-m} \quad (4)$$

and are listed in Table 2.

In-situ temperatures were measured at each site during coring operations with the APCT-3 (advanced piston corer temperature tool 3) (Collett et al., 2008). Several temperature measurements, which include seafloor temperature, were made at each site to determine the geothermal gradient. This information is also included in Table 2.

Sensitivity tests

We ran a sensitivity test to constrain the variability of Δx, Δt_1 and k_{OM} using data from Site 5C. Δx and Δt_1 are primarily constrained with the sulfate profile whereas k_{OM} was constrained with both sulfate and ammonium profiles. In this exercise we used the best fit values for Δx, Δt_1 and k_{OM}, which are 13m, 1600 years and $10^{-9.3}$ mol/m^2/sec (blue lines in Figure 3), and run the model by varying these parameters from 8 to 18m (Figure 3A), 1300 to 1900 years (Figure 3B) and from $10^{-9.5}$ to$10^{-9.1}$ mol/m^2/sec (Figure 3C). The results of this exercise indicate that our model is able to constrain the three parameters with good sensitivity and therefore it can provide a reliable quantification of the magnitude and timing of the most recent MTDs, as well as provide information on the k_{OM} in KG basin sediments.

Results and discussion

Model-estimated MTD scale and age

Our model assessment, in light of the geological background of this area, confirms our hypothesis that the S-shape sulfate profiles result from organic matter degradation driven by a rapid and recent input of fresh organic matter associated with MTDs. Our model can reproduce the observed sulfate and ammonium profiles at the seven sites where sulfate profiles indicate that the system is out of steady-state (Figure 4). The MTD thickness (Δx) and the time elapsed (Δt_1) since the mass transfer event are summarized in Table 3. We also ran the model until it reaches a new steady state after the MTD event (Figure 2D) to estimate the maximum time the anomalous sulfate profiles can survive (Δt_2). These values were listed in Table 3 as well.

The thickness of the MTDs estimated from the model ranges from 8 to 25 meters. Seismic profiles at Sites 10 and 12 image a shallow debris flow (Collett et al., 2008), which indirectly support our results, although the resolution is different from what we infer here (<25 m). High resolution multibean bathymetry profiles also document prevalent and widespread distribution of mass transfer deposits in the upper and midslope areas of the K-G basin (Ramprasad et al., 2011) with a thickness similar in magnitude to what we estimated with our model. Frequent observations of silt/sand laminae in the cores were also attributed to the influence of MTDs in the basin (Collett et al., 2008). However, our results show no correlation between the magnitude of the model-derived Δx and the frequency of laminae (Figure 4), suggesting processes other than MTD may have led to the formation of these laminae.

Using ^{14}C dating, Ramprasad et al. (2011) estimated the sediment deposition rate in one MTD to be 40 m/kyr, which is much faster than the sedimentation rate for the other hemipelagic sequence in their study (2.1 m/kyr). ^{14}C dating from Mazumdar et al. (2012) also revealed a dramatic change in sedimentation rate between two deposition modes (i.e., hemipelagic sediment rain vs. MTDs). We can estimate an average deposition rate for each mass transfer event by dividing the thickness of the slump deposit by the time elapsed since deposition ($\Delta x/\Delta t_1$) (Table 3). Our values are similar to those of Ramprasad et al. (2011) and similar or higher than those of Mazumdar et al. (2012). We also observe a positive correlation between the average deposition rate of each mass transfer event with water depth (Figure 5), if we excluded Site 15A. This correlation suggests that sites in deeper water receive more sediments than those on shallower sections of the slope, which agrees with the previous observations in this region (Ramprasad et al., 2011).

Sulfate reduction dynamics at Site 15A

At all sites except for Site 15A, the model is able to reproduce the observed ammonium and sulfate profiles using k_{OM} values ranging from $10^{-9.1}$ to $10^{-9.5}$ moles /m^2/sec. These values result in a depth-integrated POCSR rate (R_{POCSR}), which equals to the total sulfate reduction rate in the MTD section, of 149 to 623 mmol SO_4^{-2}/m^2/yr (Table 3). POC (particulate organic matter) degradation rates estimated by Wallmann et al. (2006) from the sediments of the Sea of Okhotsk and Blake Ridge range from 2.8 to 122 mmol SO_4^{-2}/m^2/yr. Dale et al. (2008) estimated the organoclastic sulfate reduction rate from the coast of Denmark to be as high as 1150 mmol SO_4^{-2}/m^2/yr. Chuang et al. (2013) recently estimated the contribution of sulfate reduction from organic matter degradation to be 4.2 to 47 mmol SO_4^{-2}/m^2/yr in southwestern offshore Taiwan. Hong et al. (2014) estimated the rates of POCSR in the sediments of Ulleung Basin to be in the range of 0.5 to 74.7 mmol SO_4^{-2}/m^2/yr. The rates we estimated for the K-G basin are on the high end of these estimates, which may be due to the fact that we estimated the R_{SR} by integrating over the 8 to 25 m-thick MTD sections. These depth sections are two to five times thicker than the typical thickness of the sulfate reduction zone, which are only a couple meters at these other sites.

The sulfate profile from Site 15A is distinctly different from the other six sites in two ways. First, the first measurement at 1.4 mbsf yielded only 8.27 mM of sulfate (Figure 4), which is significantly lower than the bottom seawater value (28 mM). Such low sulfate content together with the low initial porosity measurement (69.75% at 0.78 mbsf, Figure 6A) suggests that the top of the sediment column at this site may have been removed by a recent erosional event. Second, the drop of sulfate concentration in the upper 9 m of the hole is more dramatic compared to other sites (Figure 4). In order to match the observed, unique sulfate and ammonium profiles at Site 15A, we have to assign a distinctly higher k_{OM} that results in a higher R_{POCSR} (1215 mmol $SO_4^{-2}/m^2/yr$; Table 3) at this site. This difference may suggest that the organic matter at this site is more labile than other sites; however, the characterization of organic matter composition and provenance (Phillips and Johnson, this volume) at this site does not support this inference.

Another explanation for the higher R_{POCSR} is that the initial sulfate concentration when MTD deposited at Site 15A was not sea water value as what we assigned in the model (Figure 2B). Therefore, a R_{POCSR} similar to other sites and lower initial sulfate content can result in the current pore water profile observed at Site 15A. We hypothesized that the pore water composition of the MTD was unaltered while the sediment deposited at Site 15A. The upper portion of this MTD was later removed by another erosion event and result in the lower porosity currently observed (Figure 6A). The remaining sulfate in the intact part of the MTD was consumed by POCSR at a rate similar to other sites (Figure 6B). These combined processes result in the different sulfate profile observed at Site 15A (Figure 6C). This inference, however, assumes unchanged pore water profiles during mass transport, which does not seem to be very realistic. Although no satisfactory conclusion is arrived at this point, the combined data reveal suggest the very dynamic conditions at Site 15A.

Influence of MTDs on pore water profiles

Although only sulfate and ammonium profiles are modeled in this study, we expect MTDs to influence the distribution of all pore water species as the entire system is still in a transient state.

Therefore, any inferred reaction that assumes a steady state condition will result in erroneous conclusions and rate estimates. For example, our model results question the postulated new metabolic pathway by Schrum et al. (2009). These authors explain the low ammonium concentration observed within the first sulfate reduction zone at Site 14A as indicative of a sulfate-reducing ammonium oxidation reaction. Although their estimates of Gibbs energies for the reaction support the potential role of this metabolic process, our model clearly demonstrates that the sulfate and ammonium profiles of the K-G basin can be well explained by rapid deposition of sediment (Figure 2B), and do not necessarily require a sulfate-reducing ammonium oxidation reaction.

S-shape sulfate profiles have been reported by Hensen et al. (2003) in the west Argentine Basin. They explained such profiles as resulting from two independent slides, each of which brought a sediment package with distinct pore water compositions. The different pore water compositions from these two sediment packages, which are also different from the bottom water composition, reflect the different origins of the sediment sections. By numerically simulating this scenario, Hensen et al. (2003) concluded that the sedimentary process leading to the observed sulfate profile must have happened very recently (i.e., several tens of years). Holstein and Wirtz (2010) observed similar sulfate profiles on a tidal sand flat sediment along the northern Germany coast. They explained this observation as resulting from a rapid organoclastic sulfate reduction fueled by a downward transport of labile organic matter during flat progression. In both cases, the authors agreed upon the transient nature of the observed S-shape profiles, and propose episodic sediment pulses as their causal mechanisms. The fast sedimentation in the shallow part of sediment column rapidly buries sulfate before it diffuses out or it is entirely consumed. Such sulfate burial results in the section with almost constant sulfate concentration. If this is the only process altering sulfate profile, then “kink type” profiles of sulfate (Zabel and Schulz, 2001; Hensen et al., 2003) may be expected. Consumption of sulfate through POCSR in the section with rapid sedimentation is required for the s-shape profiles, as were observed in the K-G Basin, Argentine Basin, northern Germany coast, and potentially elsewhere along continental margins worldwide.

The MTDs inferred from our analyses of pore water data from the K-G basin are much larger in scale and significantly older than those discussed previously, which span only 2-8 meters in thickness and are thought to reflect events that occurred several tens of years before sampling

(Hensen et al., 2003 and Holstein and Wirtz, 2010). By simulating the profiles until they reach a new steady state (Figure 2D), we estimated the maximum amount of time (Δt_2) that these anomalous sulfate profiles can survive to range from 2000 to 3800 years (Table 3). Mazumdar et al. (2009) observed the similar s-shape sulfate profile from a site close to the Site 10D in our study. The rapid sedimentation for the first 6 meters of their sediment core suggests influence from MTDs which were dated as ~5 kyr old. Collectively, our results and the dating from Mazumdar et al. (2009) suggest that such S-shape sulfate profiles may survive longer than previously assumed, if MTDs are large enough in scale. The fact that we observed the influence of MTDs from the seven sites over 90 km in the basin is consistent with the observations of the widespread occurrence of MTDs in the K-G Basin. However, our modeling approach identified the influence of MTDs from some sites that were not recognized by geophysical or core observations, and points to the value of this technique in identifying MTDs and quantifying their magnitude and age.

Conclusions

By simulating the pore water sulfate and ammonium concentrations measured at seven sites drilled in the K-G Basin during the NGHP-01 expedition, we provide a quantitative description of how the MTDs can affect the geochemistry profiles. Our model provides reliable estimates of the MTDs thickness (Δx=8-25 meters), the time elapsed after the most recent event (Δt_1=450 to 1600 years), and the organoclastic sulfate reduction rate (R_{POCSR}=126 to 1215 mmol $SO_4^{-2}/m^2/yr$) at these seven sites. We also estimated the time required for the system to reach a new steady state after the MTD events (Δt_2=2000 to 3800 years).

If we exclude site 15A, we observe a positive correlation between water depth and the average depositional rate ($\Delta x/\Delta t_1$), in agreement with the previous observations of mass transport processes in this basin. The depth-integrated sulfate reduction rates estimated here are higher than published values from other sites. This is because the rates in the K-G basin were estimated by integrating over sediment depths that correspond to the thickness of the MTDs, and are two to five times thicker than the sulfate reduction zone in other studies. Site 15A is anomalous in its sulfate and porosity data which suggest that this site may be more dynamic than the other study sites.

We caution against using the pore water profiles of sites experiencing significant MTDs to infer metabolic processes before considering the role that sediment transport can have on the pore water distributions. In particular, we question the postulated sulfate-reducing ammonium oxidation pathway by Schrum et al. (2009), based on the low ammonium concentration observed within the first sulfate reduction zone at Site 14A. The results from our model show that the data at Site 14A reflects a non-steady state condition triggered by MTD in this basin.

Acknowledgement

The authors would like to thank co-chief scientists, captain, crew members and science party during the NGHP-01 expedition for their assistance with sample collection and onboard analyses. Funding support from Department of Energy (DE-FOA-0000668, DE-FE-0010496) for this work is also greatly appreciated.

References

Bastia R (2004) Depositional model and reservoir architecture of tertiary deep water sedimentation, Krishna-Godavari Offshore Basin, India. Journal of the Geological Society of India 64: 11-20

Borowski WS, Paull CK & Ussler W (1999) Global and local variations of interstitial sulfate gradients in deep-water, continental margin sediments: Sensitivity to underlying methane and gas hydrates. Marine Geology 159: 131-154

Boudreau BP (1997) Diagenetic models and their implementation: modeling transport and reactions in aquatic sediments. Springer, Berlin

Chuang PC, Dale AW, Wallmann K, Haeckel M, Yang TF, Chen NC, Chen HC, Chen HW, Lin S, Sun CH, You CF, Horng CS, Wang YS & Chung SH (2013) Relating sulfate and methane dynamics to geology: Accretionary prism offshore SW Taiwan. Geochemistry Geophysics Geosystems 14: 2523-2545

Claypool G & Kaplan I (1974) The Origin and Distribution of Methane in Marine Sediments. In: Kaplan IR (Ed) Natural gases in marine sediments (p 99). Plenum Publishing Corporation, New York

Collett T, Riedel M, Cochran J, Boswell R, Presley J, Kumar P, Sathe A, Sethi A, Lall M, Sibal V & Scientists NE (2008) Indian national gas hydrate program expedition 01 initial reports. New Delhi, India

Dale AW, Regnier P, Knab NJ, Jorgensen BB & Van Cappellen P (2008) Anaerobic oxidation of methane (AOM) in marine sediments from the Skagerrak (Denmark): II. Reaction-transport modeling. Geochimica Et Cosmochimica Acta 72: 2880-2894

Forsberg C, Solheim A, Kvalstad T, Vaidya R & Mohanty S (2007) Slope instability and mass transport deposits on the Godavari River Delta, east Indian margin from a regional geological perspective. In: Submarine Mass Movements and Their Consequences pp 19-27). Springer,

Froelich PN, Klinkhammer G, Bender Maa, Luedtke N, Heath GR, Cullen D, Dauphin P, Hammond D, Hartman B & Maynard V (1979) Early oxidation of organic matter in pelagic sediments of the eastern equatorial Atlantic: suboxic diagenesis. Geochimica et Cosmochimica Acta 43: 1075-1090

Hang PT & Brindley G (1970) Methylene blue absorption by clay minerals. Determination of surface areas and cation exchange capacities (clay-organic studies XVIII). Clays and Clay Minerals 18: 203-212

Hensen C, Zabel M, Pfeifer K, Schwenk T, Kasten S, Riedinger N, Schulz HD & Boettius A (2003) Control of sulfate pore-water profiles by sedimentary events and the significance of anaerobic oxidation of methane for the burial of sulfur in marine sediments. Geochimica et Cosmochimica Acta 67: 2631-2647

Holstein JM & Wirtz KW (2010) Organic matter accumulation and degradation in subsurface coastal sediments: a model-based comparison of rapid sedimentation and aquifer transport. Biogeosciences 7: 3741-3753

Hong WL, Torres ME, Kim JH, Choi J & Bahk JJ (2013) Carbon cycling within the sulfate-methane-transition-zone in marine sediments from the Ulleung Basin. Biogeochemistry 115: 129-148

Hong W-L, Torres ME, Kim J-H, Choi J & Bahk JJ (2014) Towards quantifying the reaction network around the sulfate-methane-transition-zone in the Ulleung Basin, East Sea, with a kinetic modeling approach. Gechimica et Cosmochimica Acta (in review)

Jaynes W & Bigham J (1987) Charge reduction, octahedral charge, and lithium retention in heated, Li-saturated smectites. Clays and Clay Minerals 35: 440-448

Kotha Y (2002) Sedimentology and sequence stratigraphy of hydrocarbon-bearing Mandapeta pays: A braided fluvial reservoir, Krishna-Godavari basin. Journal of the Geological Society of India 60: 249-270

Mazumdar A, Dewangan P, Joao HM, Peketi A, Khosla VR, Kocherla M, Badesab FK, Joshi RK, Roxanne P, Ramamurty PB, Karisiddaiah SM, Patil DJ, Dayal AM, Ramprasad T, Hawkesworth CJ & Avanzinelli R (2009) Evidence of paleo-cold seep activity from the Bay of Bengal, offshore India. Geochemistry Geophysics Geosystems 10: Q06005.

Mazumdar A, Joao HM, Peketi A, Dewangan P, Kocherla M, Joshi RK & Ramprasad T (2012) Geochemical and geological constraints on the composition of marine sediment pore fluid: Possible link to gas hydrate deposits. Marine and Petroleum Geology 38: 35-52

Murthy K (1999) Continental margin of Andhra Pradesh: Some new problems and perspectives. Visakha Science Journal 3: 21-28

Pattan JN, Parthiban G, Babu CP, Khadge NH, Paropkari AL & Kodagali VN (2008) A note on geochemistry of surface sediments from Krishna-Godavari basin, East Coast of India. Journal of the Geological Society of India 71: 107-114

Phillips SC & Johnson JE (2014) Data Report: Long-timescale particulate carbon and nitrogen variability in the Bay of Bengal and Arabian Sea. Marine and Petroleum Geology (this volume)

Prabhakar K & Zutshi P (1993) Evolution of southern part of Indian east-coast basins. Journal of the Geological Society of India 41: 215-230

Ramana M, Ramprasad T, Paropkari A, Borole D, Rao BR, Karisiddaiah S, Desa M, Kocherla M, Joao H, Lokabharati P, Gonsalves MJ, Pattan J, Khadge N, Prakash Babu C, Sathe A, Kumar P & Sethi A (2009) Multidisciplinary investigations exploring indicators of gas hydrate occurrence in the Krishna-Godavari Basin offshore, east coast of India. Geo-Marine Letters 29: 25-38

Ramprasad T, Dewangan P, Ramana MV, Mazumdar A, Karisiddaiah SM, Ramya ER & Sriram G (2011) Evidence of slumping/sliding in Krishna-Godavari offshore basin due to gas/fluid movements. Marine and Petroleum Geology 28: 1806-1816

Schrum HN, Spivack AJ, Kastner M & D'Hondt S (2009) Sulfate-reducing ammonium oxidation: A thermodynamically feasible metabolic pathway in subseafloor sediment. Geology 37: 939-942

Shanmugam G, Shrivastava SK & Das B (2009) Sandy debrites and tidalites of pliocene reservoir sands in upper-slope canyon environments, offshore Krishna-Godavari basin (India): implications. Journal of Sedimentary Research 79: 736-756

Solheim A, Forsberg C, Yang S, Kvalstad T, Longva O & Rise L (2007) The role of geological setting and depositional history in offshore slope instability. Offshore Technology Conference.

Solomon EA, Spivack AJ, Kastner M, Torres ME & Robertson G (2014) Synthesis of pore fluid geochemistry in the Krishna-Godavari Basin - Gas hydrate distribution and carbon sequestration through coupled microbial methanogenesis and silicate weathering. Marine and Petroleum Geology (this issue)

Steefel CI (2009) CrunchFlow- Software for Modeling Multicomponent Reactive Flow and Transport: User's Manual.   (p 91).

Venkatarathnam K & Biscaye PE (1973) Clay mineralogy and sedimentation in the eastern Indian Ocean. Deep Sea Research and Oceanographic Abstracts pp 727-738). Elsevier,

Von Breymann MT, Collier R & Suess E (1990) Magnesium adsorption and ion-exchange in marine-sediments - a multicomponent model. Geochimica et Cosmochimica Acta 54: 3295-3313

Von Breymann MT & Suess E (1988a) Magnesium in the marine sedimentary environment – Mg-NH4 ion-exchange. Chemical Geology 70: 359-371

Von Breymann MT, Ungerer CA & Suess E (1988b) Mg-NH4 exchange on humic-acid - a radiotracer technique for conditional exchange constants in a seawater medium. Chemical Geology 70: 349-357

Wallmann K, Aloisi G, Haeckel M, Obzhirov A, Pavlova G & Tishchenko P (2006) Kinetics of organic matter degradation, microbial methane generation, and gas hydrate formation in anoxic marine sediments. Geochimica et Cosmochimica Acta 70: 3905-3927

Wallmann K, Aloisi G, Haeckel M, Tishchenko P, Pavlova G, Greinert J, Kutterolf S & Eisenhauer A (2008) Silicate weathering in anoxic marine sediments. Geochimica et Cosmochimica Acta 72: 2895-2918

Wegener G & Boetius A (2009) An experimental study on short-term changes in the anaerobic oxidation of methane in response to varying methane and sulfate fluxes. Biogeosciences 6: 867-876

Zabel M & Schulz HD (2001) Importance of submarine landslides for non-steady state conditions in pore water systems - lower Zaire (Congo) deep-sea fan. Marine Geology 176: 87-99

Table 1: Water depth and the location of the seven study sites.

	Water Depth (m)	latitude	longitude
Site 5C	945	16° 01.722N	82° 02.677E
Site 7B	1285	16° 31.2785N	82° 40.8672E
Site 10D	1038	15° 51.8609N	81° 59.0749E
Site 12A	1038	15° 51.8609N	81° 59.0749E
Site 14A	895	16° 03.5577N	82° 05.6218E
Site 15A	926	16° 05.6983N	82° 09.7467E
Site 20A	1146	15° 48.5671N	81° 50.5760E

Table 2: Input parameters for model simulations.

	L (m)	Sea floor Temperature (°C)	Geothermal gradient (°C/m)	m	ϕ_0[b] (%)	ϕ_f[b] (%)	γ[b]	C/N	CEC[c] (meq per 100 g sed.)
Site 5C	50	7.1	0.044	2.75	77.5	57.5	-0.04	13	80
Site 7B	60	5.3	0.052	2.75	77.5	52.5	-0.04	8.5	80
Site 10D	40	6.5	0.045	3.5	77.5	63	-0.1	8.5	80
Site 12A	40	6.5[a]	0.045[a]	3.5[a]	80	60	-0.07	12	80
Site 14A	40	7.9	0.038	2.5	77	50	-0.03	13	80
Site 15A	60	7.7	0.04	2.5	70	57.5	-0.05	14	50
Site 20A	50	5.5	0.049	2.25	80	55	-0.12	10	70

[a] Assuming the same as Site 10.

[b] These parameters were estimated from the first 40 to 60 meter of the core sediments

[c] cation exchange capacity

Table 3: Model-derived results (Δx: thickness of MTD; Δt1: time elapsed after the MTD event; Δt2: times requires to reach a new steady state; k_{OM}: kinetic constant for POCSR; R_{SR}: depth-integrated sulfate reduction rate)

	Δx (m)	Δt_1 (yr)	Δt_2 (yr)	k_{OM} (10^x moles/m^2/sec)	$\Delta x/\Delta t_1$ (m/kyr)	R_{POCSR} in Δx (mmol SO_4^{-2}/m^2/yr)
Site 5C	13	1600	3350	-9.3	8.13	204
Site 7B	25	450	2200	-9.1	55.56	623
Site 10D	11	800	3800	-9.3	13.75	173
Site 12A	15	1050	2100	-9.5	14.29	149
Site 14A	13	1400	3800	-9.3	9.29	204
Site 15A	18	525	2000	-8.65	34.29	1215
Site 20A	8	300	3800	-9.3	26.67	126

Figure 1: map of the study area

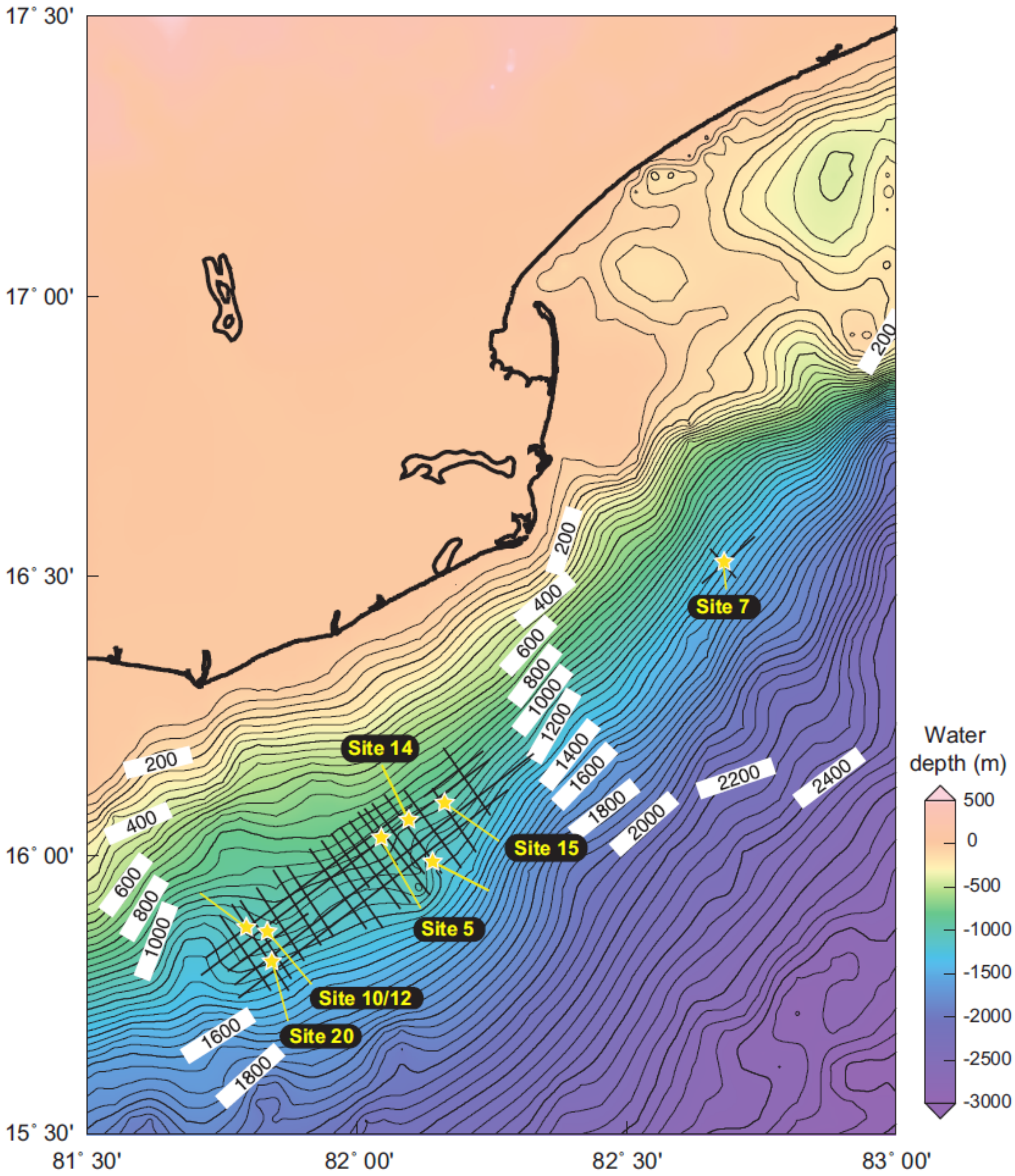

Figure 2: Schematic diagram showing the steps involved in the transport-reaction model to simulate the effect of MTDs on pore water sulfate profiles. (A) The pre-MTD pore water profiles (step 1) were set by simulating a L-meter long sediment column to steady state using sea water composition as the initial condition. Methane flux assigned here is constrained by the both sulfate and methane profiles (i.e., the assigned methane flux has to be at least higher than the observed flux). (B) The MTD (the grey rectangle) with fresh labile organic matter is deposited instantaneously onto the sediment column and buries the SMTZ to a greater depth. (C) In step 2, the pore water profiles and methane flux resulting from step 1 are used as the initial condition. Due to the addition of reactive labile organic matter in the MTD, sulfate is consumed at shallow depth through POCSR only (the first sulfate reduction zone) whereas methane exhausts sulfate from below by AOM and POCSR (the second sulfate reduction zone). The SMTZ in (B) and (C) illustrate this non-steady-state condition, which is observed at seven KG basin sites. The Δx (thickness of MTD) and Δt_1 (time required to reach present observed profile) are estimated by fitting data at each site and are reported in Table 3. (D) The system is expected to reach another new steady state condition after Δt_2 years (Table 3).

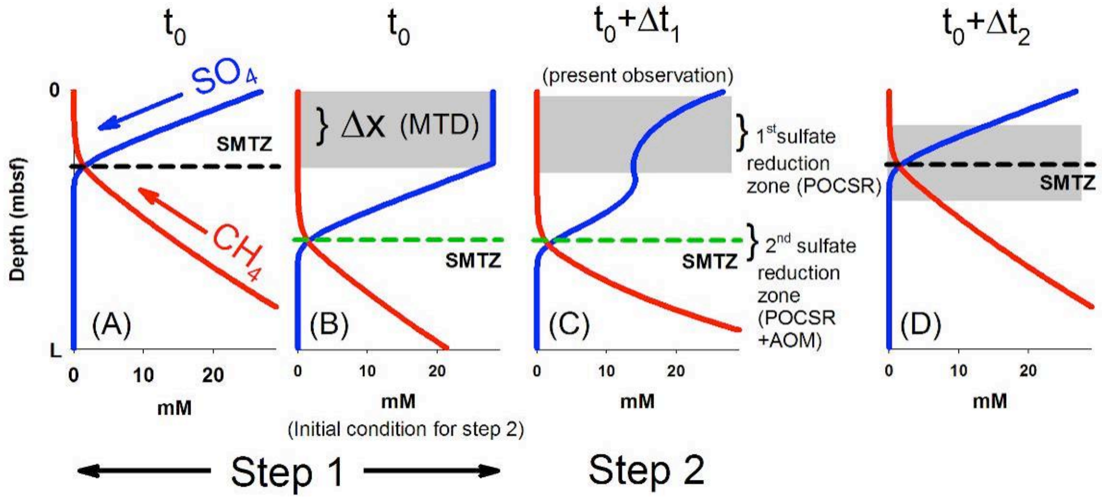

Figure 3: Simulation conducted at Site 5C to test the sensitivity of the model to the Δx, Δt and k_{OM} parameters. Blue lines in each panel indicate the best fit to the data, and red lines show changes that would result from small variations in the values assigned to these parameters As the results indicate, the three parameters can be well constrained by fitting the observed sulfate and ammonium profiles.

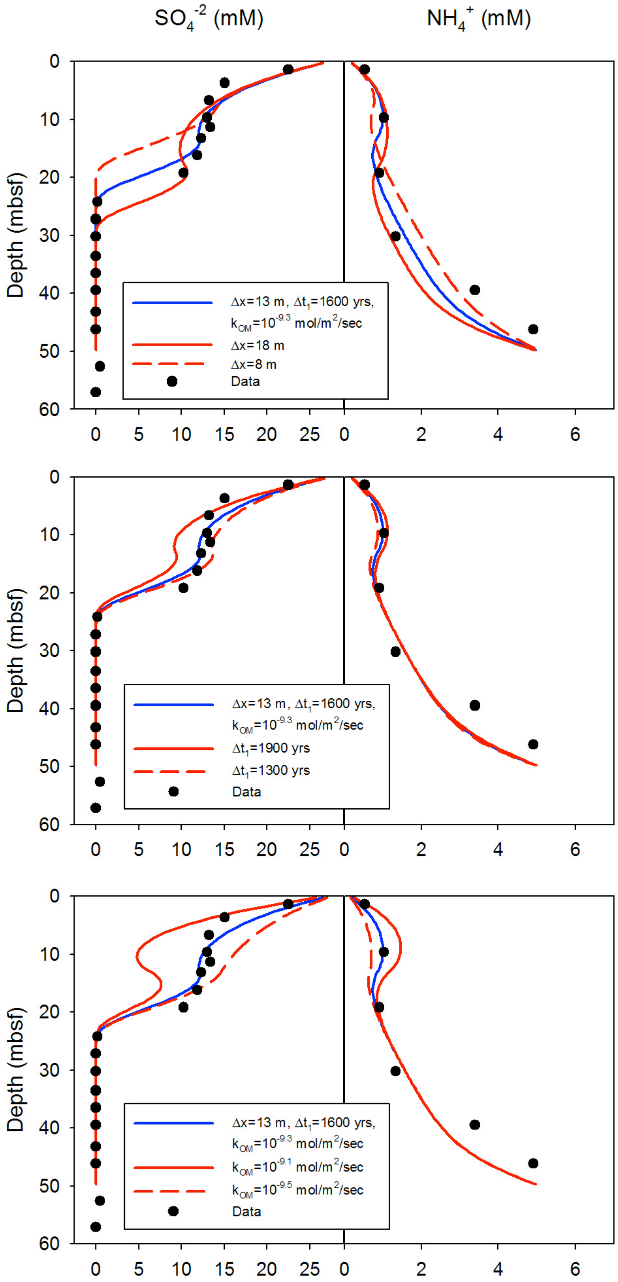

Figure 4A: Model results and the observed sulfate (blue lines and circles), methane (red lines and squares), and ammonium (pink lines and diamonds) profiles at the seven study sites. The depths where thin silt laminae and beds (grey lines) were observed at each site were also plotted for comparison although no apparent correlation was observed between the frequency of laminae and the thickness of MTDs (Δx, Green lines).

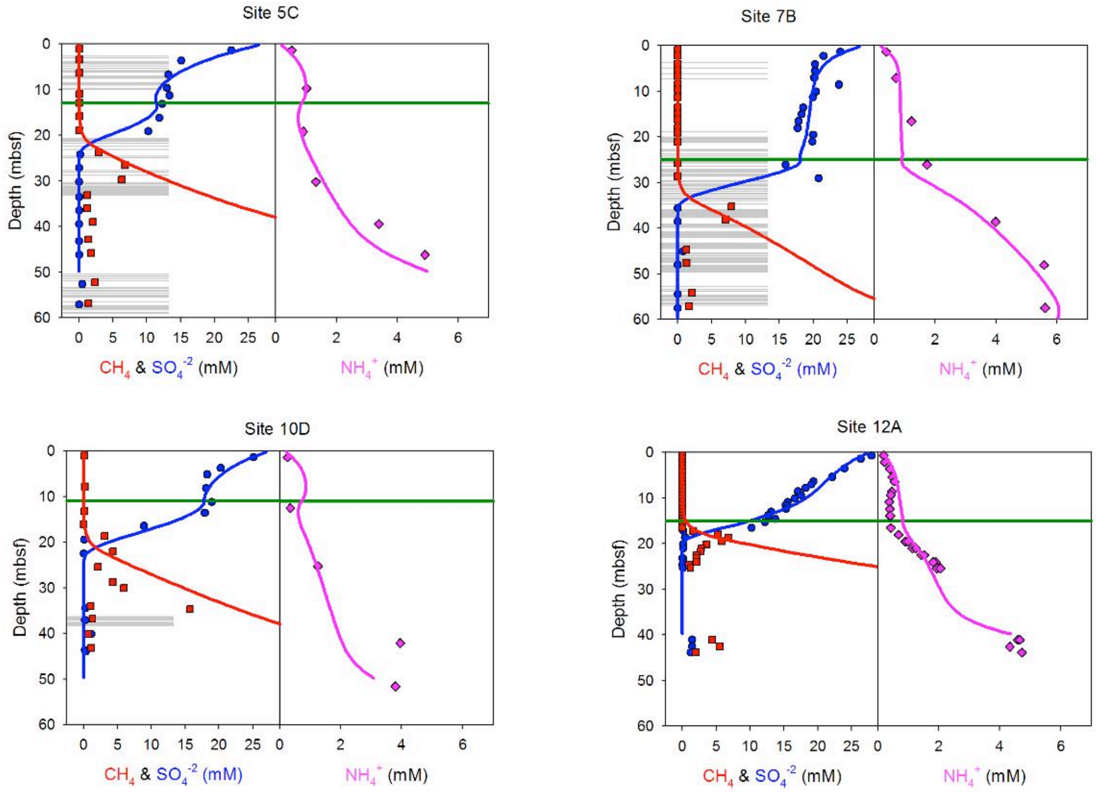

Figure 4B

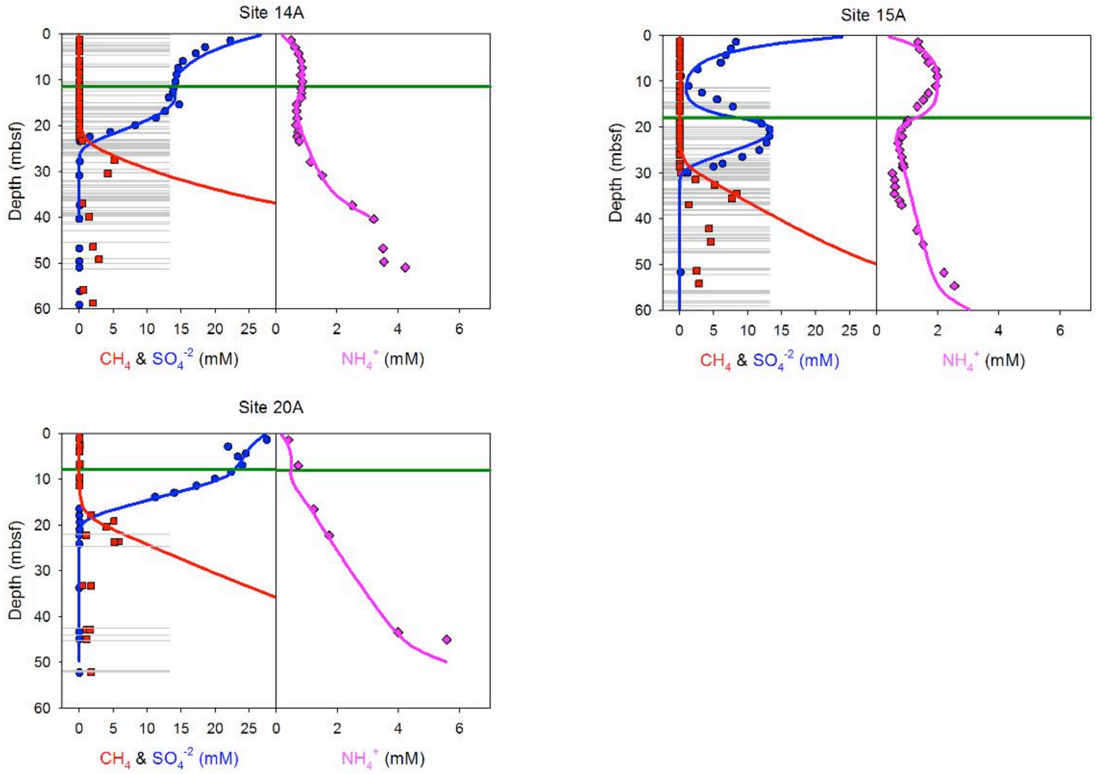
Site 14A
Site 15A
Site 20A
Depth (mbsf)
0
10
20
30
40
50
60
0 5 10 15 20 25
0 2 4 6
CH4 & SO4-2 (mM)
NH4+ (mM)

Figure 5: Correlation between water depth and the average depositional rate ($\Delta x/\Delta t$). The positive correlation, if Site 15A is excluded, suggests that sites at greater water depth receive more sediments than those located in shallower water which agrees with previous observation in this region (Ramprasad et al., 2011). In order to fit the sulfate profile in Site 15A, a higher k_{OM} is required which may suggest more dynamic conditions at this site as described in the text.

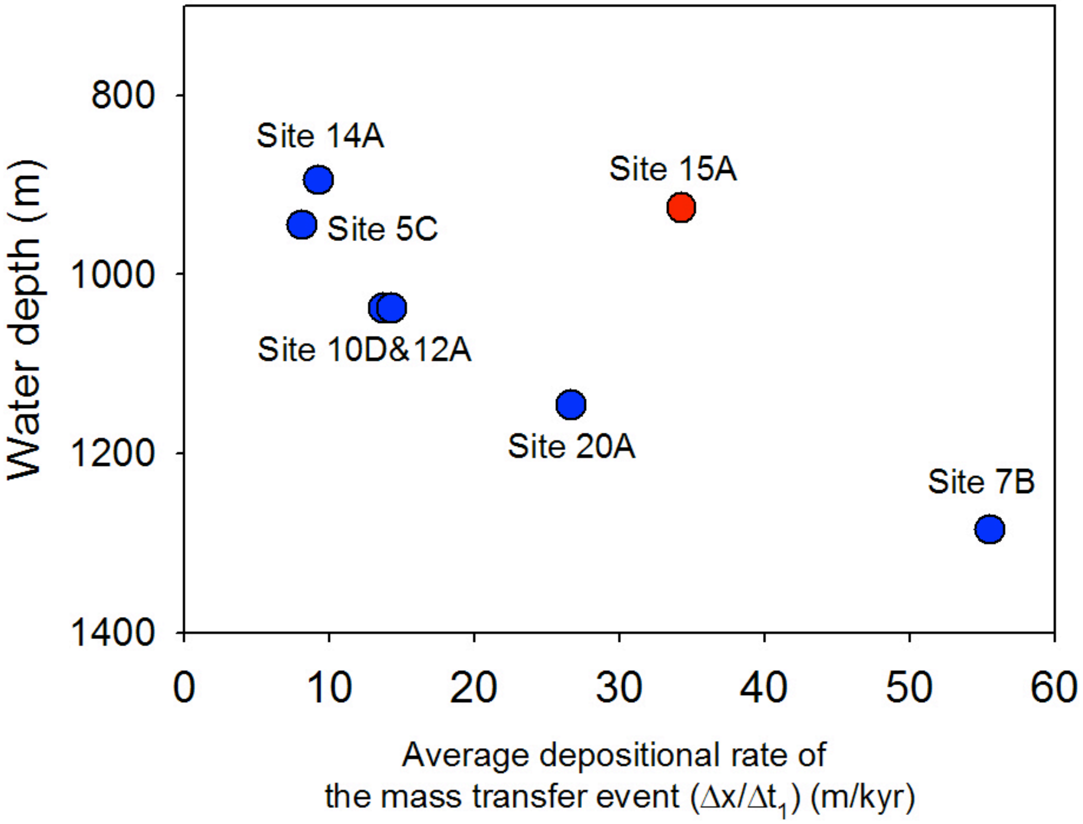

Figure 6: Conceptual model to exaplain the sulfate profile at Site 15A. (A) Comparison of porosity profiles between Site 14A and 15A, the two adjacent sites. The first measurement at Site 15A is ~5% lower than that at Site 14A suggesting that the MTD section in Site 15A may have undergone recent erosion. The two red lines mark our estimated thickness of MTD at Site 15A. In contrast to the initial homogenous sulfate content in the MTD sections at all other sites (Figure 2B), the intial sulfate profile in the MTD section at Site 15B may already be low in sulfate and the total depletion of sulfate within the MTD suggests that this sediment column had experienced POCSR for a period of time before the emplacement at Site 15A. Such that immediately after emplacement, the system had a sulfate distribution as shwon in (B) The continuous consumption of sulfate by POCSR in the MTD section after depositing result in the present observed sulfate profile at Site 15A, as shown in (C)

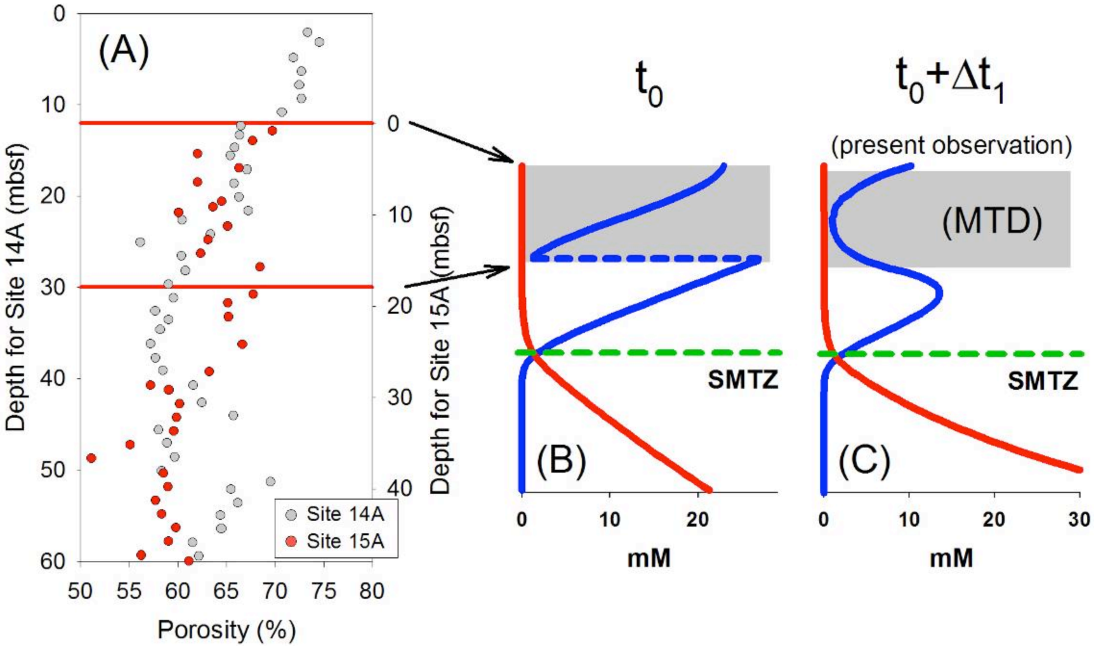

National Energy Technology Laboratory

626 Cochrans Mill Road
P.O. Box 10940
Pittsburgh, PA 15236-0940

3610 Collins Ferry Road
P.O. Box 880
Morgantown, WV 26507-0880

13131 Dairy Ashford, Suite 225
Sugarland, TX 77478

1450 Queen Avenue SW
Albany, OR 97321-2198

2175 University Ave. South
Suite 201
Fairbanks, AK 99709

Visit the NETL website at:
www.netl.doe.gov

Customer Service:
1-800-553-7681

DEPARTMENT OF ENERGY • UNITED STATES OF AMERICA